Surface Science 83 (1979) 45–59

A STUDY OF THE KINETICS OF THE INTERACTIONS OF O_2 AND N_2O WITH A Cu(111) SURFACE AND OF THE REACTION OF CO WITH ADSORBED OXYGEN USING AES, LEED AND ELLIPSOMETRY

F.H.P.M. HABRAKEN, E.Ph. KIEFFER and G.A. BOOTSMA
Van 't Hoff Laboratory, University of Utrecht, Padualaan 8, 3584 CH Utrecht, The Netherlands

Received 19 September 1978

The interactions of O_2 and N_2O in the low pressure range with a Cu(111) surface and of CO with adsorbed oxygen have been studied with ellipsometry, Auger electron spectroscopy and LEED. The adsorption of O_2 was investigated in the 10^{-6}–10^{-4} Torr range and at crystal temperatures ranging from 23 to 400°C. O_2 chemisorbs dissociatively with an initial reaction probability of about 10^{-3} and an apparent activation energy of 2–4 kcal/mol, which depends on the substrate temperature, up to a saturation coverage of 0.45. The probability of decomposition of N_2O is 10^{-5} at 300°C, and the activation energy is 10.4 kcal/mol for $250 < T < 400$°C. The oxygen coverage saturates at $\theta = 0.45$ as well. For both oxidation reactions the kinetics can be described with a precursor state model. With LEED no superstructures were observed. The probability of the reaction of CO with adsorbed oxygen is 4×10^{-5} at 250°C and is initially independent of the oxygen coverage. The reaction is assumed to proceed via a Langmuir–Hinshelwood mechanism. The activation energy for the reaction $CO_{ad} + O_{ad} \rightarrow CO_2$ is 18–20 kcal/mol.

1. Introduction

Knowledge and understanding of the role of the surface geometry in the kinetics of the reactions of gases with metal surfaces is important for catalysis. The interactions of oxygen and certain oxygen containing gases with copper surfaces of various orientations are at present being studied with ellipsometry, Auger electron spectroscopy and LEED. In contrast to techniques which use electrons or ions as probes, the optical technique of ellipsometry makes possible in-situ kinetic measurements at high pressures without interference with the processes under investigation. Furthermore, the difference in information depth between AES and ellipsometry permits a distinction to be made between surface and subsurface phenomena.

The interaction of molecular oxygen with large single crystals, films and small particles of copper at pressures between 10^{-8} and 200 Torr has been the subject of many investigations, e.g. with LEED [1–5], AES [5], UPS [6,7], XPS [7], SIMS [8], work function measurements [5,6,9] and gas volumetry [10–12]. However, kinetic studies are scarce and the results differ widely. At room temperature the

sticking coefficient s of O_2 on surfaces of large crystals was found to be of the order of 10^{-3}–10^{-2} and to depend on the structure of the surface [1–5,8,9]. At room temperature s turned out to be about an order in magnitude lower for Cu(111) than for Cu(110) and Cu(100). Contrary to (110) and (100) no superstructures are formed on (111) after exposures up to 5×10^4 L (1 Langmuir = 10^{-6} Torr s = 1.33×10^{-4} Pa s) [1–4]. Adsorption measurements on films yielded $s \approx 0.1$ [6,11].

In the experimental conditions bulk oxides (Cu_2O, CuO) are thermodynamically stable, and unlike with large single crystals, with small copper particles they are readily formed; this may be ascribed to the local temperature increase caused by the evolution of the high heat of adsorption (~110 kcal/mol [10,12,13]). Ellipsometric results on the oxidation of copper surfaces at higher pressures have been reported [14,15], but no data in the submonolayer range have been presented.

A nitrous oxide molecule N_2O decomposes on a Cu surface into N_2, which desorbs, and into an adsorbed oxygen atom [2,10,13,16]. The LEED patterns formed after decomposition of N_2O are the same as upon adsorption of O_2, except for the (100) plane [2]. The N_2O reaction is much slower at room temperature and strongly activated, and even with small copper particles no oxide formation takes place at temperatures up to ~120°C. Above this temperature oxidation of copper powder has been observed at pressures of 200–600 Torr [10,16].

At room temperature CO is only weakly adsorbed (heat of adsorption 10–15 kcal/mol, cf. refs. [17–19]). In his LEED study of the interaction of CO with oxygen preadsorbed on Cu(111), Ertl observed no changes in a superstructure ascribed to oxygen at temperatures up to 550°C, in contrast to the other low-index Cu-planes [20].

In the present paper results are presented of a study of the adsorption of O_2 on Cu(111), the decomposition of N_2O and the removal reaction with CO (10^{-6}–10^{-3} Torr, crystal temperatures 23–400°C). A preliminary account of this work has been presented in ref. [21].

2. Experimental

The experiments were performed in a Varian UHV system (VT 114 B) provided with facilities for LEED–AES, ellipsometry, quadrupole mass-spectrometry and ion bombardment. The experimental arrangement was designed so that the available surface techniques could be applied without changing the position of the crystal. The system is analogous to that described in refs. [22,23], except for the presence of a poppet valve between the reaction chamber and the ion and sublimation pump unit. The working chamber was evacuated with a 70 l/s turbomolecular pump, a 240 l/s integrated ion pump and titanium sublimation unit and usually reached a pressure of a few times 10^{-10} Torr after bake-out at 200°C for about 60 h. After closure of the poppet valve the pressure rose to about 10^{-8} Torr. Then the mass-

spectra showed distinct peaks for m/e = 28 (CO, 88%) and 44 (CO_2, 8%).

The gas handling system was pumped by the turbomolecular pump to a pressure lower than 10^{-6} Torr. The gases used, i.e. argon (purity 99.999%), oxygen (99.995%), carbon monoxide (99.0%), nitrous oxide (99.99%) and carbon dioxide (99.997%) were purchased from L'Air Liquide. Check experiments were done with high purity carbon monoxide (99.997%). During all exposures the gas in the reaction chamber was continuously renewed by pumping with the turbomolecular pump.

The sample was a disc-shaped crystal (diameter 6.5 mm, thickness 2.6 mm) spark-cut to within 2° of the (111) orientation from a 5N copper rod from the Material Research Corporation. After grinding and electro-lap-polishing, the crystal was mounted in a stainless-steel sample holder, which could be heated to about 700°C with a resistance wire placed at the back of the crystal. The temperature was measured with a chromel–alumel thermocouple attached to the edge of the crystal. After the procedure of polishing had been repeated the results could be reproduced. The surface was cleaned by cycles of sputtering (typically 600 eV Ar^+, 5 $\mu A/cm^2$, angle of incidence ~45°, 30 min) and annealing (450°C, 15 min). When only oxygen was left on the surface, an exposure of CO of about 3×10^4 L at 350°C was sufficient to clean the surface.

The ellipsometric arrangement and procedure was as described in ref. [24] (wavelength 632.8 nm, angle of incidence 68.6 ± 0.3°). Most of the static ellipsometric measurements were done in two zones. Changes in Δ during transient phenomena were followed by off-null irradiance measurements. The polarizer was deliberately set at about three degrees off-compensation and the analyser was set at compensation, so that the change in transmitted irradiance was approximately proportional to the change in Δ. The measured $\delta\Delta$, $\delta\Delta \equiv \bar{\Delta} - \Delta$ ($\bar{\Delta}$: clean surface), was checked by two-zone measurements before and after an experiment.

The Auger spectra were taken with a four grid retarding field analyser (RIBER, OPR 304). The angle of incidence of the primary electron beam was 7 ± 1° with the plane of the surface, the beam energy was 2500 eV and its current 8 μA. The modulation voltage was 12 V p–p.

3. Determination of oxygen coverage

In the submonolayer range a linear relationship was found between $\delta\Delta$ and the ratio h_O/h_{Cu} of the oxygen 510 eV to the copper 920 eV peak-to-peak heights in the second derivative Auger spectra (fig. 1). At the highest coverage the attenuation of the Cu 63 and 920 eV Auger peaks was of the order of 10%. These results strongly suggest that $\delta\Delta$ is proportional to the oxygen coverage. It should be pointed out that similar relationships were obtained for oxygen on Ag(110) [25] and Cu(110) [26] at room temperature. In this range for Cu(111) the change in the other ellipsometric parameter $\delta\psi \approx 1/3\ \delta\Delta$.

An experimental absolute coverage calibration has been obtained for oxygen on

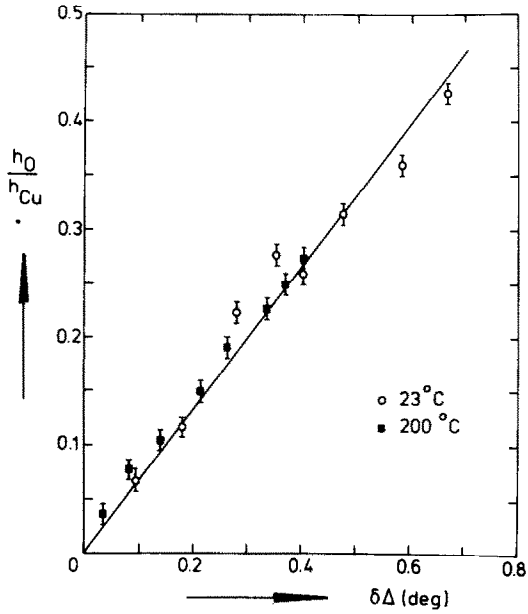

Fig. 1. Ratio of the O 510 eV to the Cu 920 eV peak versus $\delta\Delta$ upon adsorption of oxygen on Cu(111) at 23°C and upon removal of adsorbed oxygen with CO at 200°C.

Cu(110), where a simple (2 X 1) LEED pattern is observed [26]. If one takes θ = 0.5 (O atoms/Cu surface atom) for the (2 X 1) superstructure, a comparison of the h_O/h_{Cu} values yields, after correction for the difference in atomic density of the planes, for Cu(111):

$$\theta = (0.65 \pm 0.06)\,\delta\Delta\,. \qquad (1)$$

In this calibration it is assumed that the Cu 920 eV Auger signal is equal for Cu(110) and Cu(111). This was conformed by measuring the absolute peak-to-peak heights of the Cu 920 eV signal for both planes. It should be pointed out that the above assumption has also been confirmed recently for the Ni 848 eV peak for Ni(100) and Ni(110) [27].

4. Interaction of O_2 and N_2O with Cu(111)

4.1. Adsorption of oxygen

Oxygen adsorption curves were taken at crystal temperatures from room temperature up to 400°C with off-null irradiance measurements. Some examples are presented in fig. 2. The oxygen pressures were in the 10^{-6}–10^{-5} Torr range, where

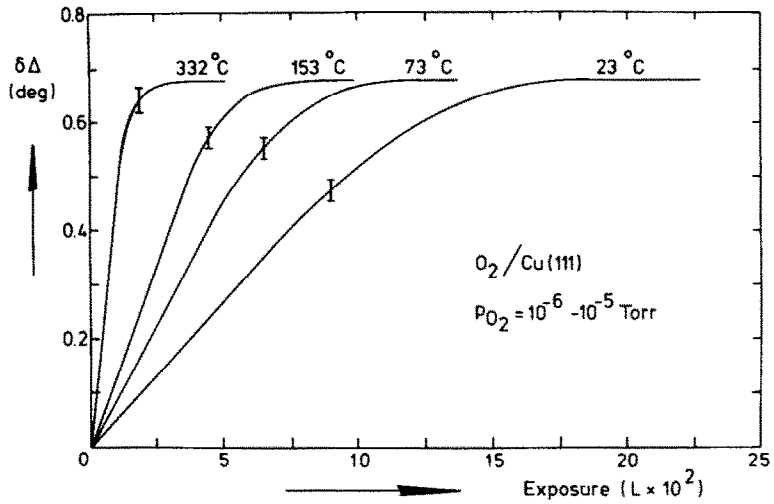

Fig. 2. $\delta\Delta$ versus exposure of oxygen to a clean and annealed Cu(111) surface (experimental errors indicated).

the background gas (mainly CO) could be neglected. The rate of adsorption appeared to be proportional to the oxygen pressure.

A saturation effect was observed at $\delta\Delta_{sat} = 0.68 \pm 0.02°$. With a hot filament or at temperatures above 175°C a further, much slower change in Δ took place, which was only measurable at pressures above 10^{-4} Torr. (For slow processes it was difficult to distinguish between changes in Δ and mechanical drift of the sample holder.) In this second oxidation stage the ellipsometric parameter ψ and the oxygen Auger signal remained nearly constant. In view of the difference in information depth between AES (0.6 nm) and ellipsometry (14 nm), these data can be ascribed to incorporation of oxygen into the copper lattice (see section 5). In our experimental conditions the rate of change of Δ for the second stage was $>10^3$ times slower than that for the chemisorption stage. In this paper we consider only the kinetics associated with the first chemisorption stage in detail.

Up to saturation the LEED patterns showed no extra spots but only an increase in background intensity. At all temperatures evacuation caused no change in Δ.

4.2. Decomposition of N_2O

The decomposition of N_2O on a Cu(111) surface has been investigated in the temperature region 250–400°C at pressures mainly above 10^{-4} Torr. Oxygen coverages were determined both with AES and ellipsometry. In all cases no nitrogen could be detected in the Auger spectra, which confirms that the overall reaction is $N_2O \rightarrow N_2 \uparrow + O_{ad}$. It was necessary to switch off the ion pressure gauge to prevent

the formation of large amounts of NO on the hot filament (according to mass-spectra). The pumping speed after an exposure with the ion gauge on was strongly reduced, which is known to occur with NO in a stainless steel chamber [28].

Adsorption curves for different temperatures are represented in fig. 3. The Auger measurements were done in the region where ellipsometric measurements took too much time because of the instability of the sample holder.

The ellipsometric curves were determined with off-null irradiance measurements. The difference between the curves taken with AES and with ellipsometry at $T \approx 320°C$ for $\theta > 0.2$ is probably due to the reaction of adsorbed oxygen with NO produced on the hot filament of the ion gauge and/or the Auger electron gun before and during the recording of an Auger spectrum ($p < 10^{-8}$ Torr). Upon exposure with the pressure gauge switched on the oxygen coverage remained low. A saturation effect was observed at the same oxygen coverage as upon chemisorption of O_2. As with O_2 the LEED patterns showed no extra spots, only an increase in background intensity.

4.3. Adsorption of CO_2 and CO

With ellipsometry and AES no interaction of CO_2 with a clean or an oxygen-covered Cu(111) surface was observed up to pressures of 10^{-3} Torr at 24 and 364°C (exposures $\leq 5 \times 10^5$ L), when the ion gauge was switched off. A hot fila-

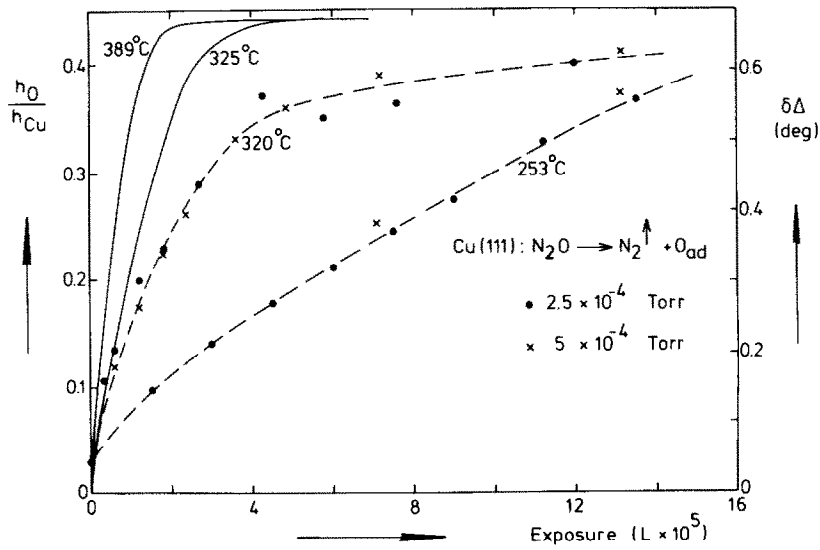

Fig. 3. δΔ (solid lines) and oxygen Auger signal (dots and crosses) versus exposure of N_2O to Cu(111).

ment caused the formation of CO (1–2%), then after the CO_2 exposure the pumping speed was reduced.

Within the detection limit of AES and ellipsometry ($\theta \approx 0.03$) no adsorption or disproportionation of CO was observed on a clean Cu(111) surface up to $T = 460°C$ (exposures $\leqslant 3 \times 10^5$ L).

4.4. Discussion

The initial sticking coefficient $s(0)$ for O_2 is of the order of 10^{-3} at 23°C and increases with the temperature of the crystal. This value is intermediate between values reported for Ni(111) (~1 [29]) and Ag(111) (~3×10^{-5} [30]). In fig. 4 the sticking coefficient is depicted as a function of the coverage at different temperatures; $s(\theta)$ remains constant up to $\theta \approx \frac{1}{2}\theta_{sat}$. According to eq. (1) the oxygen saturation coverage (θ_{sat}) shown in figs. 2 and 3 is 0.45 ± 0.05. From the fact that $\theta_{sat} \approx \frac{1}{2}$ and is the same for O_2 and N_2O it can be concluded that in both cases the adsorption site per oxygen atom consists of two nearest-neighbour (nn) copper atoms.

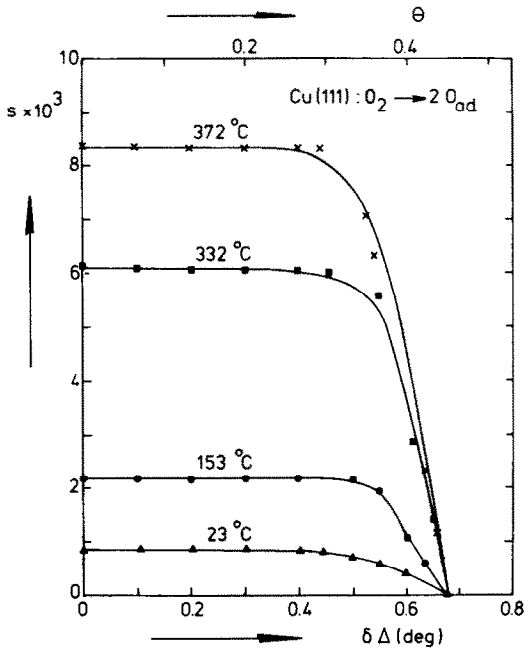

Fig. 4. Oxygen sticking coefficient s versus $\delta\Delta$, derived from ellipsometric measurements. The solid lines represent eq. (2) with $r(\theta') = r(0)$; $K_1 = 0.018$ and $K_2 = 0.98$ at 23°C and $K_1 = 0.010$, $K_2 = 1.00$ at 153, 332 and 372°C.

This already suggests that the oxygen molecules are dissociatively adsorbed (for further evidence see section 5). The LEED patterns indicate that the adsorption takes place in a disordered, random fashion.

The data in fig. 4 could be fitted with the equation derived by Kohrt and Gomer [31] for dissociative adsorption via a precursor state requiring a pair of adjacent free sites:

$$\frac{s(\theta')}{s(0)} = \frac{1-r(\theta')}{1-r(0)}\frac{s'(\theta')}{s'(0)} = \frac{1-r(\theta')}{1-r(0)}\left(1+K_1\frac{\theta'}{1-\theta'}+K_2\theta'\right)^{-1}(1-\theta'), \tag{2}$$

where $\theta' = \theta/\theta_{sat}$, r is the reflection probability of gas molecules and s' the probability for chemisorption of accommodated precursor molecules. The constants K_1 and K_2 are related to the probabilities for chemisorption (P_a) and for desorption of the precursor molecules from empty chemisorption sites (P_d), from filled sites (P'_d) and from sites not available for chemisorption, e.g. a single site in the case of dissociative adsorption (P''_d):

$$K_1 = P'_d/(P_a+P_d) \quad \text{and} \quad K_2 = 1 - P''_d/(P_a+P_d)\,. \tag{3}$$

Chemisorption is assumed to take place after dissociation of the mobile precursor, e.g. physisorbed oxygen molecules. In the derivation of eq. (2) it is assumed that the distribution of filled sites is random, i.e. that the chemisorbed oxygen atoms are mobile, and that lateral interactions between them may be neglected. Adsorption stops when no free adsorption site (i.e. two free nn substrate atoms) is left. With highly mobile atoms one expects $\theta_{sat} = \frac{1}{2}$. When the atoms are immobile θ_{sat} will become <0.5, because part of the non-occupied substrate atoms will only have occupied nn atoms. With restricted mobility it will take long before the final coverage of $\frac{1}{2}$ is reached. Our measurements yielded $\theta_{sat} = \frac{1}{2}$ within experimental accuracy, justifying the use of eq. (2).

The fits in fig. 4 were obtained by assuming that the reflection probability r is independent of θ. From the results ($K_1 \approx 10^{-2}$ and $K_2 \approx 1$) and eq. (3) it follows that P'_d and P''_d are small ($\sim 10^{-2}$). If also P_d would be small,

$$s'(0) = P_a/(P_a+P_d) \approx 1\ ;$$

this means that on a free site every physisorbed O_2 molecule dissociates and becomes chemisorbed, and that $1-r \approx 10^{-3}$. The experimentally observed increase in $s(0)$ with increasing temperature would imply that r decreases with increasing temperature, which is not very probable (cf. N_2/W(100) system [32]). So one must conclude that in contrast to P'_d and P''_d, P_d will have an appreciable value.

A recent molecular beam study showed that the assumption of r being independent of θ does not apply to the interaction of O_2 with Pd(111) [33]. By assigning a different reflection probability to empty and filled sites (r_1 and r_2), one gets $r(\theta) = r_1(1-\theta) + r_2\theta$ and instead of eq. (2) [31]:

$$\frac{s(\theta')}{s(0)} = \frac{s'(\theta')}{s'(0)}\left(1+\theta'\frac{r_1-r_2}{1-r_1}\right). \tag{4}$$

In the absence of molecular beam data for O_2 on Cu, a fit with this equation has not been attempted because of the large number of adjustable parameters.

The Arrhenius plot of $s(0)$ (fig. 5) shows that the apparent activation energy, E_{act}, increases with increasing crystal temperature. Phenomenologically two regions could be distinguished: $T < 230°C$ with $E_{act} = 1.7$ kcal/mol and $230 < T < 400°C$ with $E_{act} = 4$ kcal/mol. In the precursor model the activation energy should be interpreted as the difference between the energy barriers for chemisorption and desorption of fully accommodated precursor molecules, if r is independent of T. The change in E_{act} could be due to a change in r; the $s(\theta)$ curves give no indication for the occurrence of two different processes in the two temperature regions. Unfortunately, in this study we could not vary the temperature of the gas phase and were therefore unable to obtain additional information.

Fig. 6 shows the reaction probability of N_2O, defined as the number of adsorbed oxygen atoms per incident N_2O molecule. The solid lines are the best fits with the equation for adsorption on a single site via a precursor state [31], for r independent of θ:

$$\frac{s(\theta')}{s(0)} = \left(1 + K_1 \frac{\theta'}{1-\theta'}\right)^{-1} . \tag{5}$$

The absolute value of $s(0)$ is about 10^{-5} at 300°C and increases with the crystal temperature. The Arrhenius plot (fig. 7) shows a straight line for the temperature range studied (250–400°C), $s(0) = A \exp(-E_{act}/RT)$, with $E_{act} = 10.4 \pm 0.6$ kcal/

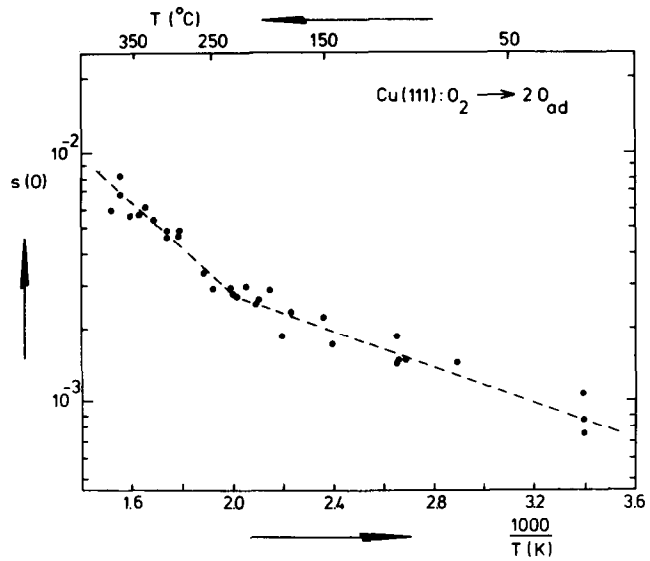

Fig. 5. Arrhenius plot of $s(0)$ for O_2 on Cu(111).

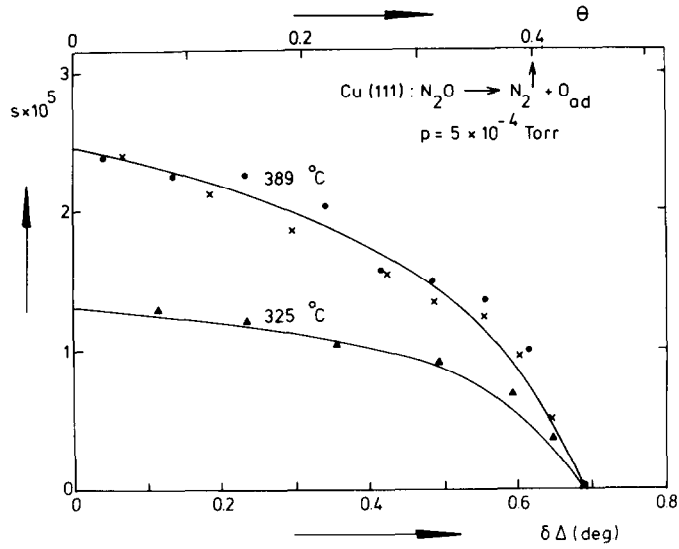

Fig. 6. Reaction probability s for the N_2O decomposition on Cu(111) as a function of $\delta\Delta$ (oxygen coverage), derived from ellipsometric measurements. The solid lines represent eq. (5) with $K_1 = 0.2$ at 325°C and $K_1 = 0.3$ at 389°C.

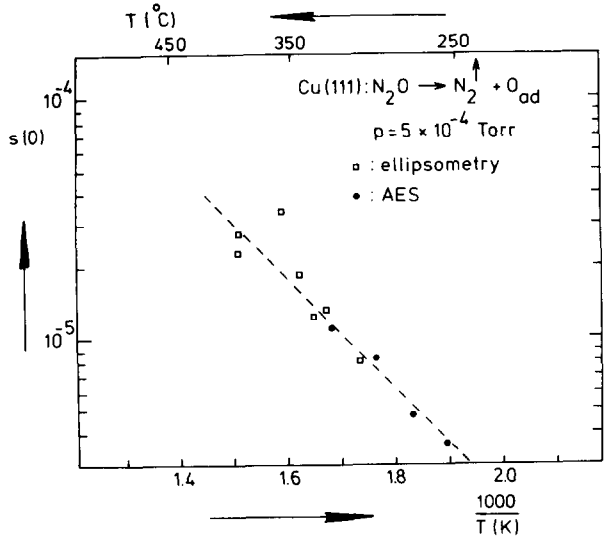

Fig. 7. Arrhenius plot of $s(0)$ for the decomposition of N_2O on Cu(111).

mol and $A = 0.09$. Extrapolation to room temperature gives $s(0) \approx 10^{-9}$. This very low value is in qualitative agreement with the value deduced from ref. [10] for the decomposition of N_2O on copper powder ($\sim 10^{-11}$).

5. The reaction of CO with preadsorbed oxygen

It appeared possible to reduce an oxidized surface by means of CO at higher crystal temperatures. Exposures of CO to a surface saturated with adsorbed oxygen ($\delta\Delta = \delta\Delta_{sat} = 0.68°$) were carried out in the pressure range 5×10^{-5}–5×10^{-4} Torr with the crystal temperatures ranging from 200 to 460°C. The presence of a hot filament caused an increase in the reaction probability of CO with O_{ad} with about a factor of 2, so the exposures were made with the ionisation gauge switched off.

Fig. 8 shows to typical plots of $\delta\Delta$ as a function of CO exposure. The removal of oxygen from a more strongly oxidized surface ($\delta\Delta = 1.1°$) is represented in fig. 9. The simultaneous AES and ellipsometric measurements show that apparently during the first stage the surface concentration of oxygen remains constant. After reduction of the surface with CO a small amount of oxygen ($\theta \approx 0.04$) was generally still present, as measured with AES. This may have been caused by readsorption of oxygen during evacuation before and during an AES-spectrum was taken or by the presence of more strongly bound oxygen. This effect became more serious after a long series of experiments.

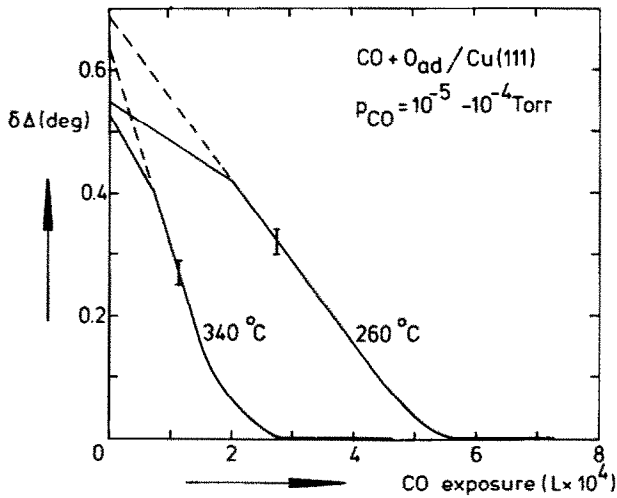

Fig. 8. $\delta\Delta$ versus exposure of CO to a surface with preadsorbed oxygen ($\delta\Delta = 0.68$). Off-null irradiance measurements.

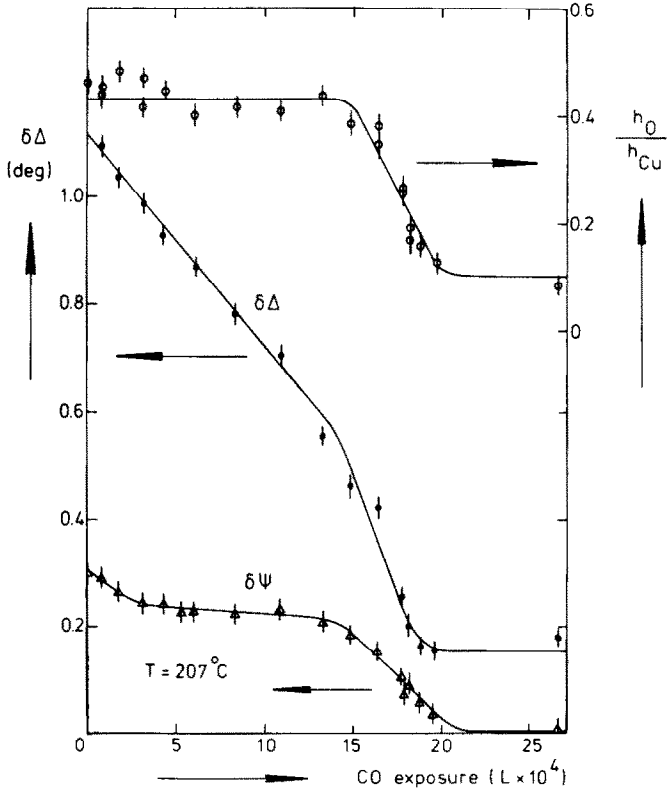

Fig. 9. Interaction of CO with oxygen adsorbed at 200°C and 2×10^{-4} Torr (1.2×10^5 L). Upper curve: AES measurements; other curves: ellipsometric two-zone measurements. During the measurements the exposure was interrupted.

The kinetic curves for the reaction of CO with sorbed oxygen show two distinct stages (figs. 8 and 9) with a constant ratio of 2.3 for the slope $d\delta\Delta/dt$.

From fig. 9 it can be concluded that the second stage is associated with the lowering of the surface oxygen concentration. At the same temperature the slopes of the first stage are, within experimental accuracy, equal for the continuous and the interrupted measurements. In fig. 8 linear extrapolation of the second stage to the start of the exposures yields approximately $\delta\Delta_{sat}$.

During both stages $d\delta\Delta/dt$ is proportional to the CO pressure. The Arrhenius plot of $(-1/P_{CO})$ $(d\delta\Delta/dt)$ shows to straight lines (fig. 10), which run parallel. Obviously during both stages the same process is rate limiting, this process being probably the removal of oxygen from the surface. During the first stage the empty surface site must then immediately be filled up by oxygen from beneath the surface. The resulting effect is that oxygen is removed from the selvedge. The differ-

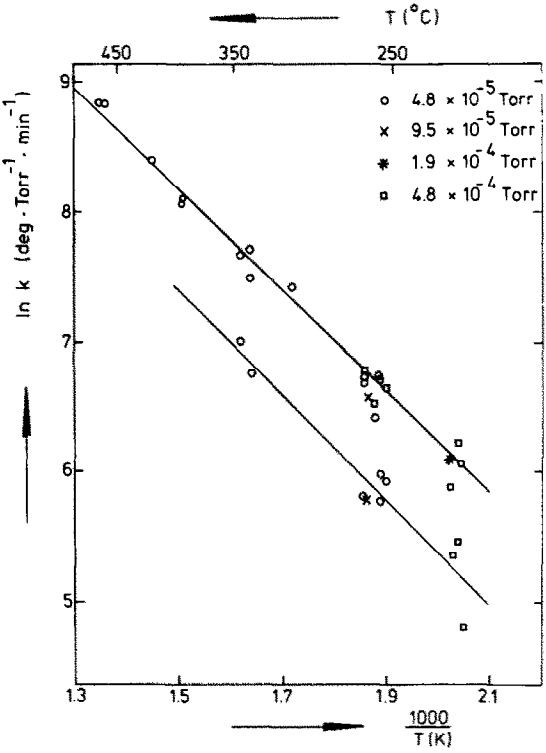

Fig. 10. Arrhenius plot of the reaction coefficient k for the removal of oxygen by CO. Lower curve: first stage; upper curve: second stage (see text).

ence in slope then represents the difference in sensitivity of the ellipsometer to surface- and bulk-oxygen. It is noteworthy that ψ does not change during the first stage of reduction just as during the second stage of oxidation (section 4.1). Apparently after deposition of half a monolayer of oxygen, in the time between the adsorption and reduction experiments (typically 2 h) adsorbed oxygen moves into the selvedge and a fixed part ($\sim\frac{2}{3}\,\theta_{sat} = 0.3$) remains on the surface. Attempts to follow this incorporation process directly were not successful because of the lack of stability of the sample holder at the higher temperatures. When the time between oxidation and reduction was taken small (~15 min) the ellipsometer showed no change in Δ during evacuation, but then with CO the second stage only was observed.

In view of the uncertainty in the interpretation of ellipsometric data the experimental results for the second stage of oxidation and the first stage of reduction could alternatively be explained by assuming restructuring of the surface at a constant oxygen coverage. However, one then has to introduce a number of less proba-

ble assumptions with respect to the influence of oxygen and CO on the rearrangement of the atoms in the interfacial region.

The reaction coefficient $k \equiv (-1/P_{CO})\ (d\delta\Delta/dt)$ is independent of the oxygen coverage down to 0.15 θ_{sat}. The Arrhenius plots of k yield an activation energy of 8.0 ± 0.6 kcal/mol. At 250°C the initial reaction probability (number of oxygen atoms removed per incident CO molecule) is 4×10^{-5}.

Because k is strongly dependent on the temperature but initially independent of the oxygen coverage, one must conclude that in the overall reaction $CO + O_{ad} \rightarrow CO_2 \uparrow$, the reacting CO molecules are also adsorbed on the surface (Langmuir–Hinshelwood mechanism) and that they are mobile (cf. ref. [34]). The heat of adsorption of CO on Cu(111) has been reported to be 10–12 kcal/mol [18,19]. Thus the equilibrium concentration of CO_{ad} will vary as exp(10–12 kcal/mol/RT) and is expected to be very small in the range of temperatures and pressures of our study. For the activation energy of the rate-limiting step, $CO_{ad} + O_{ad} \rightarrow CO_2$, we get 18–20 kcal/mol.

No difference in reduction rate was observed between surface oxygen originating from O_2 or N_2O. This is a clear indication that O_2 dissociates upon chemisorption.

6. Conclusions

(i) Ellipsometry has proved to be a suitable technique for the study of the kinetics of oxidation and reduction of Cu(111). Its combination with AES permits to distinguish between different processes at or near the surface.

(ii) Oxygen chemisorbs dissociatively via a precursor state. At room temperature the initial sticking probability is $\sim 10^{-3}$. The chemisorption stage saturates at $\theta = 0.45$. An apparent activation energy of 1.7 kcal/mol for $23 < T < 230$°C and 4 kcal/mol for $230 < T < 460$°C has been found.

(iii) The deposition of atomic oxygen via the decomposition of N_2O also leads to a saturation coverage of 0.45 in the temperature range 250 to 400°C. The initial reaction probability is about 10^{-5} at 300°C and the activation energy 10.4 kcal/mol. The kinetics can also be described with a precursor state model.

(iv) The reaction of CO with preadsorbed oxygen is assumed to proceed via a Langmuir–Hinshelwood mechanism with an activation energy for the reaction $CO_{ad} + O_{ad} \rightarrow CO_2$ of 18–20 kcal/mol. The initial reaction probability is 4×10^{-5} at 250°C.

Acknowledgements

The authors thank Mr. A.H.J. Huijbers for technical assistance. The investigations were supported by the Netherlands Foundation of Chemical Research (SON) with financial aid from the Netherlands Organization for the Advancement of Pure Research (ZWO).

References

[1] G. Ertl, Surface Sci. 6 (1967) 208.
[2] G.W. Simmons, D.F. Mitchell and K.R. Lawless, Surface Sci. 8 (1967) 130.
[3] A. Oustry, L. Lafourcade and A. Escaut, Surface Sci. 40 (1973) 545.
[4] L. McDonnell and D.P. Woodruff, Surface Sci. 46 (1974) 505.
[5] P. Hofmann, R. Unwin, W. Wyrobisch and A.M. Bradshaw, Surface Sci. 72 (1978) 635.
[6] L.F. Wagner and W.E. Spicer, Surface Sci. 46 (1974) 301.
[7] S. Evans, D.E. Parry and J.M. Thomas, Faraday Disc. Chem. Soc. 60 (1975) 102.
[8] A. Müller and A. Benninghoven, Surface Sci. 41 (1974) 493.
[9] T.A. Delchar, Surface Sci. 27 (1971) 11.
[10] J.J.F. Scholten and J.A. Konvalinka, Trans. Faraday Soc. 65 (1969) 2465.
[11] E. Fromm, H. Duppel and U. Bauder, Thin Solid Films 33 (1976) 323.
[12] A.A. Vasilevich, G.P. Shpiro, A.M. Alekseev, T.A. Semenova, J.M. Markina, T.A. Vasil'eva and O.G. Budkina, Kinetics and Catalysis 16 (1976) 1363.
[13] R.M. Dell, F.S. Stone and F.P. Tiley, Trans. Faraday Soc. 49 (1953) 195.
[14] F.W. Young, J.V. Cathcart and A.T. Gwathmey, Acta Met. 4 (1956) 145.
[15] R.W. Stobie, B. Rao and M.J. Dignam, Surface Sci. 56 (1976) 334.
[16] Th. Osinga, B.G. Linsen and W.P. van Beeck, J. Catalysis 7 (1967) 277.
[17] J. Pritchard, J. Vacuum Sci. Technol. 9 (1972) 895.
[18] H. Conrad, G. Ertl. J. Küppers and E.E. Latta, Solid State Commun. 17 (1975) 613.
[19] J. Kessler and F. Thieme, Surface Sci. 67 (1977) 405.
[20] G. Ertl, Surface Sci. 7 (1967) 309.
[21] F.H.P.M. Habraken, E.P. Kieffer and G.A. Bootsma, in: Proc. 7th Intern. Vacuum Congr. and 3rd Intern. Conf. on Solid Surfaces (Vienna, 1977) p. 877.
[22] F.C. Schouten, E.W. Kaleveld and G.A. Bootsma, Surface Sci. 63 (1977) 460.
[23] H. Albers, Thesis, Univ. of Utrecht (1978).
[24] H. Albers, J.M.M. Droog and G.A. Bootsma, Surface Sci. 64 (1977) 1.
[25] H. Albers, W.J.J. van der Wal, O.L.J. Gijzeman and G.A. Bootsma, Surface Sci. 77 (1978) 1.
[26] F.H.P.M. Habraken and G.A. Bootsma, Ned. Tijdschr. Vacuum Tech. 16 (1978) 142.
[27] F.C. Schouten, E. te Brake, O.L.J. Gijzeman and G.A. Bootsma, Surface Sci. 74 (1978) 1.
[28] R. Ku, N.A. Gjostein and H.P. Bonzel, Surface Sci. 64 (1977) 465.
[29] P.H. Holloway and J.B. Hudson, Surface Sci. 43 (1974) 141.
[30] H. Albers, W.J.J. van der Wal and G.A. Bootsma, Surface Sci. 68 (1977) 47.
[31] C. Kohrt and R. Gomer, J. Chem. Phys. 52 (1970) 3283.
[32] D.A. King and M.G. Wells, Proc. Roy. Soc. (London) A339 (1974) 245.
[33] T. Engel and G. Ertl, in: Proc. 7th Intern. Vacuum Congr. and 3rd Intern. Conf. on Solid Surfaces (Vienna, 1977) p. 1365; J. Chem. Phys. 69 (1978) 1267.
[34] T. Matsushima, D.M. Almy and J.M. White, Surface Sci. 67 (1977) 89.